

## Using Heterocycle to Improve the Selectivity of Rhodamine-6G Dye: Synthesis of Pyrrole-Modified Rhodamine-6G and its Recognition to Zn<sup>2+</sup>

<sup>1,2</sup>Rui Qiao\*, <sup>1</sup>Hai-Yun Fan, <sup>1,2</sup>Cui-Bing Bai\*\*, <sup>1</sup>Ling Dai, <sup>1,2</sup>Lin Zhang, <sup>1</sup>Jie Zhang,  
<sup>1,2</sup>Shui-Sheng Chen and <sup>1,2</sup>Hui Miao

<sup>1</sup>School of Chemistry and Materials Engineering, Fuyang Normal University,  
Fuyang, Anhui Province, 236037, China.

<sup>2</sup>Anhui Province Key Laboratory for Degradation and Monitoring of Pollution of the Environment,  
236037, China.

qiaorui@mail.ipc.ac.cn\*; baicuibing@126.com\*\*

(Received on 1<sup>st</sup> March 2018, accepted in revised form 26<sup>th</sup> September 2018)

Summary: The fluorescent sensor XQN for Zn<sup>2+</sup> based on rhodamine-6G have been designed and synthesized. XQN showed fluorescent specific selectivity and high sensitivity for Zn<sup>2+</sup> against other metal ions such as Fe<sup>3+</sup>, Cr<sup>3+</sup>, Hg<sup>2+</sup>, Ag<sup>+</sup>, Ca<sup>2+</sup>, Cu<sup>2+</sup>, Pb<sup>2+</sup>, Cd<sup>2+</sup>, Ni<sup>2+</sup>, Co<sup>2+</sup> and Mg<sup>2+</sup> in CH<sub>3</sub>CN-PBS(phosphate buffer saline) (10 mM, v/v=7:3, pH = 7.4) solution. The distinct color change and the rapid emergence of fluorescence emission provided naked-eyes detection for Zn<sup>2+</sup>. The test strip results showed that these sensors could act as a convenient and efficient Zn<sup>2+</sup> test kit. The recognition mechanism of the sensor toward Zn<sup>2+</sup> was evaluated by IR and the Job's plots. The detection limits of XQN towards Zn<sup>2+</sup> was calculated as 2.39 μM. In addition, XQN-Zn<sup>2+</sup> fluorescence lifetime and fluorescence quantum yield were also measured.

**Keywords:** Rhodamine-6G; Pyrrole; The fluorescent sensor; Zn<sup>2+</sup>; Test kit.

### Introduction

In recent decades, the exploration of selective and sensitive fluorescent sensors for the detection of transition metal ions have been received great attention [1-6]. Amongst the important transition metal ions, Zn<sup>2+</sup> is known for their ability in comprehensive applications. And Zn<sup>2+</sup> plays a critical role in biological, environmental and chemical systems [7-10]. Nevertheless, the disruption of Zn<sup>2+</sup> is very dangerous to human health. For example, the imbalance of Zn<sup>2+</sup> has been strongly linked to hypoxia ischemia, epilepsy, amyotrophic lateral sclerosis, and several neurological disorders including Parkinson's disease and Alzheimer's disease [11-13]. So, it is highly desirable and absolutely necessary to develop the effective method to detect Zn<sup>2+</sup> [14-16].

Fluorescent sensors, which are capable of recognizing guest species sensitively and sensitively, are of particular interest in supramolecular chemistry to check trace amount of transition metal ions in the last decades [17, 18]. The research efforts have been focused on the design and practical application of novel sensors because of their high selectivity and low cost.

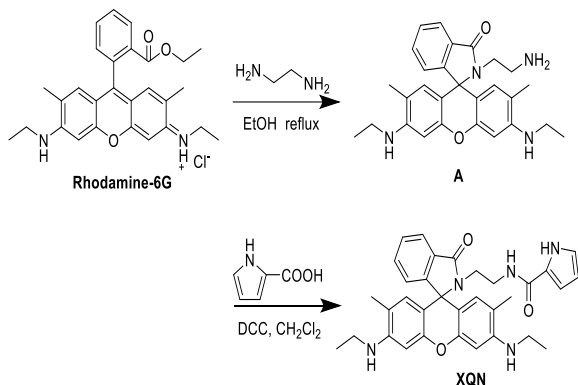
It is well known for the favourable spectroscopic properties of rhodamine derivatives that include large absorption coefficient, high

fluorescence quantum yield, long absorption and emission wavelength [19]. In particular, the modified spirolactam structure which enables colorless and nonfluorescent can be transformed into the colored and highly fluorescent ring-opened amide form in the presence of the corresponding metal ions [20]. Because of the particular "off-on" interaction mechanism, rhodamine derivatives have become the prior choice in constructing novel sensors, especially for the transition metal ions such as Zn<sup>2+</sup>. In order to increase the sensitivity and selectivity to the metal ions, some heterocycles have been used to modify the rhodamine platform, such as furan, pyrrole and thiophene [21, 22]. However, most of them are obtained through C=N by aromatic aldehydes reacting with *N*-(rhodamine-B) lactam-ethylenediamine or *N*-(rhodamine-B) lactam-hydrazine hydrate [23-25]. But few compounds linked by amide between heterocycles and rhodamines have been reported. And it is clear that the derivatives modified by amide have more potential coordination sites to bind Zn<sup>2+</sup> than by C=N unit, which may strengthen sensitivity and selectivity.

In this paper, the novel rhodamine-based fluorescent chemosensor XQN was designed and synthesized (Scheme-1), which was modified by pyrrole structure with amide to improve increase the selectivity of rhodamine-6G dye. To our surprised, the rhodamine derivative could "naked-eye"

\*To whom all correspondence should be addressed.

recognize  $Zn^{2+}$  with high selectivity and specific sensitivity in  $CH_3CN$ -PBS (phosphate buffer saline) (10 mM, v/v=7:3, pH=7.4). Meanwhile, other cations such as  $Fe^{3+}$ ,  $Cr^{3+}$ ,  $Hg^{2+}$ ,  $Ag^+$ ,  $Ca^{2+}$ ,  $Cu^{2+}$ ,  $Pb^{2+}$ ,  $Cd^{2+}$ ,  $Ni^{2+}$ ,  $Co^{2+}$  and  $Mg^{2+}$  could not cause any interference.



Scheme-1: Synthetic route to fluorescent sensor XQN.

## Experimental

### General spectroscopic methods

All UV-vis spectroscopy and fluorescent spectroscopy were carried out on a Shimadzu UV-1601 spectrometer and a HORIBA FLUOROMAX-4-NIR spectrometer. The concentration of XQN was kept constantly ( $3.3 \times 10^{-4}$  M). The solution of metal ions were prepared from the nitrates salts of  $Fe^{3+}$ ,  $Cr^{3+}$ ,  $Hg^{2+}$ ,  $Ag^+$ ,  $Ca^{2+}$ ,  $Cu^{2+}$ ,  $Pb^{2+}$ ,  $Cd^{2+}$ ,  $Ni^{2+}$ ,  $Co^{2+}$  and  $Mg^{2+}$ .

$^1H$  NMR and  $^{13}C$  NMR spectra were performed on a Bruker at 400 MHz using TMS as an internal standard,  $DMSO-d_6$  as the solvents. Melting points were measured on an X-4 digital melting-point apparatus (uncorrected). Infrared spectra were obtained on a Nicolette 5700 FT-IR spectrophotometer. Mass spectra were carried on with a Shimadzu LCMS-IT/TOF mass spectrometer. Solvents were purified and dried using standard protocol, the other chemical reagents were obtained commercially and used as received without further purification. All reagents were used of analytical grade.

### Synthesis of compound XQN

The synthesis of compound XQN was outlined in Scheme-1. According to the reported procedure, compound A was synthesized [17, 26]. Pyrrole-2-carboxylic acid (0.01 mol), DCC (0.02 mol) and A (0.01 mol) were dissolved in  $CH_2Cl_2$  (10 mL) in a 25 mL round-bottom flask. The reaction mixture was stirred for 12 h at room temperature. When the solvent was evaporated under reduced pressure, the crude product

was purified by silica gel chromatography (ethyl acetate: petroleum ether = 1: 2) to obtain the fluorescent sensor XQN. *N*-(2-(3',6'-bis(ethylamino)-2',7'-dimethyl-3-oxospiro[isindoline-1,9'-xanthen]-2-yl)ethyl)-1*H*-pyrrole-2-carboxamide (XQN): Yield 83%, m.p. >300 °C,  $^1H$  NMR ( $DMSO-d_6$ , 400 MHz)  $\delta$  11.34 (s, 1H), 7.92-7.72 (m, 2H), 7.56-7.38 (m, 2H), 7.03-6.90 (m, 1H), 6.79 (dd,  $J=3.9, 2.6$  Hz, 1H), 6.61 (d,  $J=3.5$  Hz, 1H), 6.27 (s, 2H), 6.13 (s, 2H), 6.01 (dd,  $J=5.9, 2.4$  Hz, 1H), 5.06 (t,  $J=5.4$  Hz, 2H), 3.28-3.04 (m, 6H), 2.92 (dt,  $J=11.7, 5.9$  Hz, 2H), 1.86 (s, 6H), 1.22 (t,  $J=7.1$  Hz, 6H).  $^{13}C$  NMR (100 MHz,  $DMSO$ )  $\delta$  167.85, 160.80, 157.05, 154.36, 151.42, 148.11, 133.20, 130.51, 128.67, 127.85, 126.50, 124.05, 122.81, 121.64, 118.74, 110.05, 108.89, 104.88, 96.18, 64.81, 33.82, 17.48, 14.64. HRMS (ESI)  $m/z$ :  $[M+H]^+$  Calcd for  $C_{33}H_{35}N_5O_3$ : 550.2813; Found 550.2816.

## Results and Discussion

The optical responses of compound XQN to various metal cations including  $Fe^{3+}$ ,  $Cr^{3+}$ ,  $Hg^{2+}$ ,  $Ag^+$ ,  $Ca^{2+}$ ,  $Zn^{2+}$ ,  $Cu^{2+}$ ,  $Pb^{2+}$ ,  $Cd^{2+}$ ,  $Ni^{2+}$ ,  $Co^{2+}$  and  $Mg^{2+}$  was investigated in  $CH_3CN$ -PBS (10 mM, v/v=7:3, pH=7.4) through UV-vis and fluorescence spectroscopic methods. Firstly, free sensor XQN was colorless and no absorption was detected above 500 nm in UV-vis spectrum. When adding  $Zn^{2+}$  to the XQN solution, XQN immediately responded with dramatic color changes from colorless to yellow-green (Fig. 1). And a new absorption peak appeared at 525 nm. It might be due to the structure transformation from spirolactam to the ring-opened amide form with adding  $Zn^{2+}$ . To validate the selectivity to different metal ions, the same tests were investigated in use of  $Fe^{3+}$ ,  $Cr^{3+}$ ,  $Hg^{2+}$ ,  $Ag^+$ ,  $Ca^{2+}$ ,  $Cu^{2+}$ ,  $Pb^{2+}$ ,  $Cd^{2+}$ ,  $Ni^{2+}$ ,  $Co^{2+}$  and  $Mg^{2+}$  instead of  $Zn^{2+}$  by UV-vis spectroscopy. Although  $Fe^{3+}$  and  $Hg^{2+}$  also led to color changes, their changes are less pronounced than  $Zn^{2+}$ . The results exhibited that XQN could discriminate  $Zn^{2+}$  from other ions.

In addition, the fluorescent properties of XQN in the presence of various cations were studied. The sensor did not display any appreciable emission excited at 525 nm. However, the fluorescence spectra of sensor XQN dramatically changed along with the  $Zn^{2+}$  concentration increase. For sensor XQN, an intense emission peak arose at 550 nm (Fig. 2). As a result, the fluorescent intensity at 550 nm was enhanced gradually with the increase of  $Zn^{2+}$  concentration (Fig. 3). Although the emission peak of  $Fe^{3+}$  and  $Hg^{2+}$  also appeared at 550 nm the same as  $Zn^{2+}$ , the fluorescent peak of sensor XQN at 550 nm was strongest caused by  $Zn^{2+}$  (Fig. 2). It was considered that the nonfluorescent spirolactam was transformed into the high fluorescent ring-open amide form when  $Zn^{2+}$  was added.

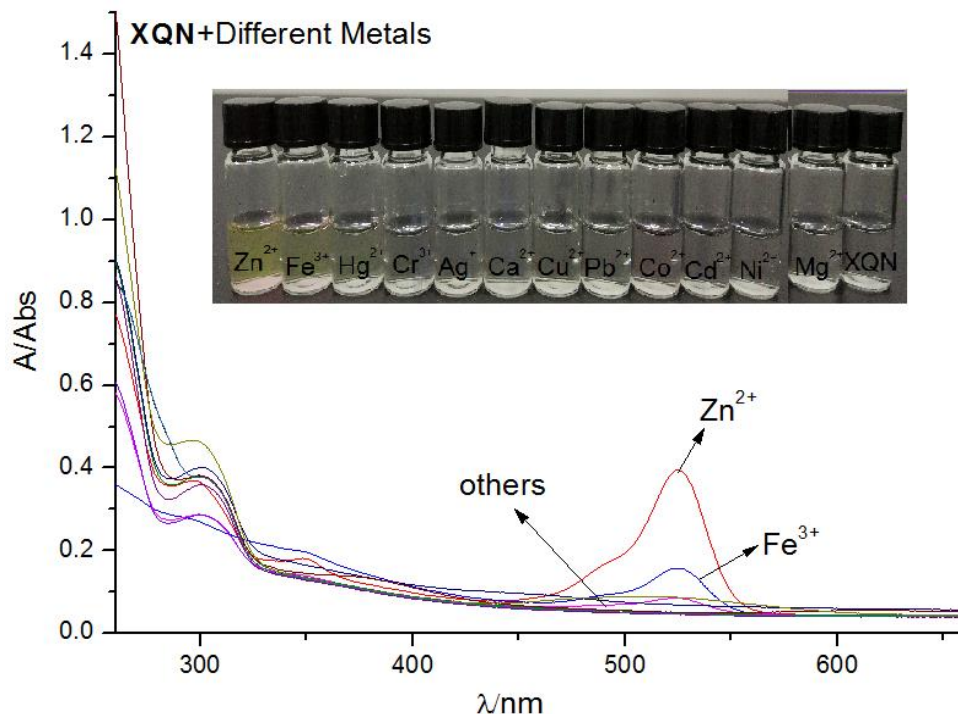


Fig. 1: Absorption spectra of the sensor XQN ( $3.3 \times 10^{-4}$  M) in the presence of various metal ions in  $CH_3CN$ -PBS (10 mM, v/v=7:3, pH = 7.4). Inset: Photographs of chemosensor XQN ( $3.3 \times 10^{-4}$  M) in the presence of various metal ions in  $CH_3CN$ -PBS (10 mM, v/v=7:3, pH = 7.4).

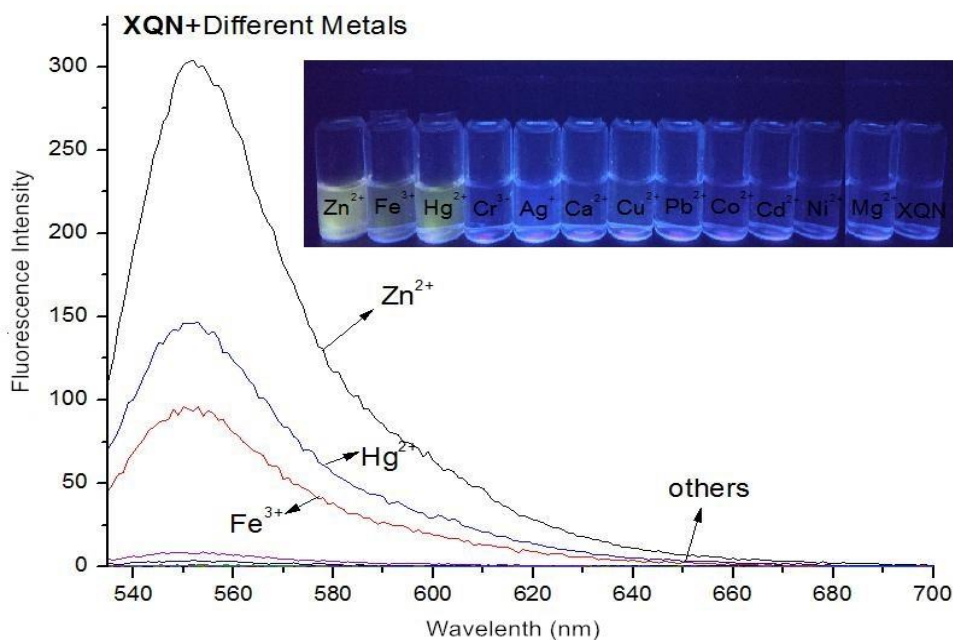


Fig. 2: Fluorescence spectra changes of the sensor XQN ( $3.3 \times 10^{-4}$  M) in the presence of various metal ions in  $CH_3CN$ -PBS (10 mM, v/v=7:3, pH = 7.4),  $\lambda_{ex} = 525$  nm, detection from 540 to 720 nm. Inset: Photographs of chemosensor XQN ( $3.3 \times 10^{-4}$  M) in the presence of various metal ions in  $CH_3CN$ -PBS (10 mM, v/v=7:3, pH = 7.4)

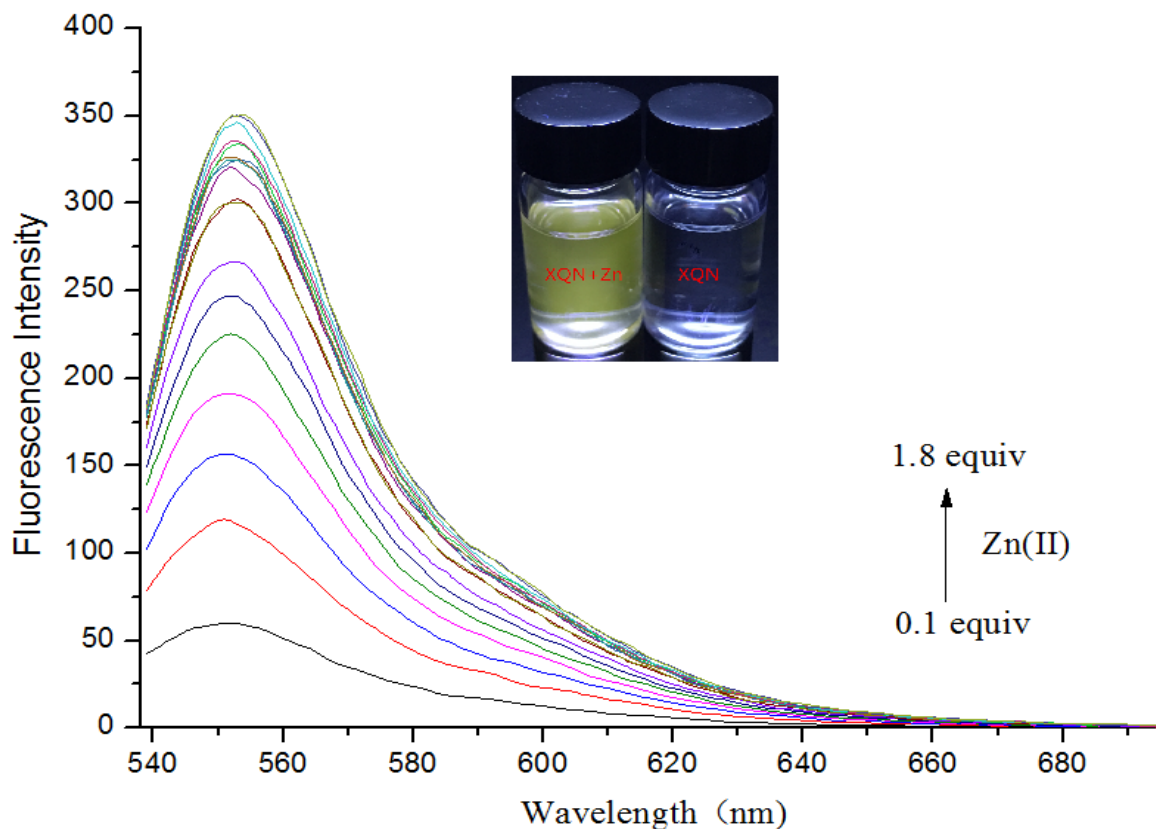


Fig. 3: Fluorescence spectra of XQN ( $3.3 \times 10^{-4}$  M) in the presence of different concentration of  $Zn^{2+}$  (0-1.8 equiv.) in  $CH_3CN$ -PBS (10 mM, v/v=7:3, pH=7.4),  $\lambda_{ex} = 525$  nm, detection from 540 to 700 nm.

To further exploit the utility of sensor XQN, competitive experiments were carried out (Fig. 4). The results indicated that the recognition of sensor XQN towards  $Zn^{2+}$  was hardly affected by coexistent cations. And it also suggested that XQN could be used as a potential fluorescent sensor for  $Zn^{2+}$ . Moreover, the changes in the fluorescence intensity at 550 nm depending on the reaction time were recorded from 0 to 60 min (see SI Fig. S4). The experimental results confirmed that the fluorescence intensity significantly increased immediately when 20 equivalents of  $Zn^{2+}$  solution was added to the solution of sensor XQN ( $3.3 \times 10^{-4}$  M). And it clearly showed that the reaction completed quickly after  $Zn^{2+}$  was added into the solution of sensor XQN.

To confirm the stoichiometry of the binding of sensor with  $Zn^{2+}$  as well as the mechanism of interaction between XQN and  $Zn^{2+}$ , the Job's plots analyses and IR analyses were conducted [26, 27]. As the main object, the Job's plots of sensors XQN clearly showed that the maximum fluorescence intensity at 550 nm with a mole fraction at 0.5 which indicated that the stoichiometric ratio of the

interaction between them was 1: 1 (see SI Fig. S5 and Fig. 6).

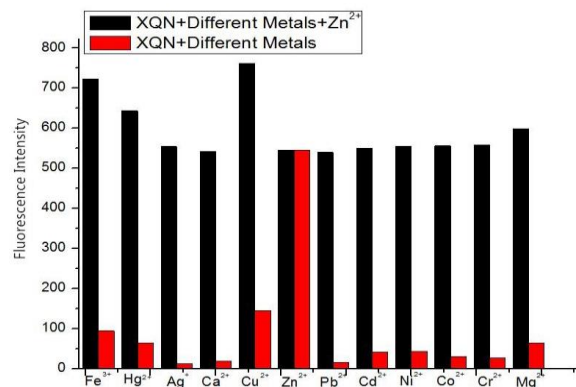


Fig. 4: Fluorescence response of XQN ( $3.3 \times 10^{-4}$  M) in  $CH_3CN$ -PBS (10 mM, v/v=7:3, pH = 7.4) at 550 nm upon addition of respective metal ions, followed by addition of  $Zn^{2+}$  (1.5 equiv.),  $\lambda_{ex} = 525$  nm. The anti-interference of XQN ( $3.3 \times 10^{-4}$  M) for  $Zn^{2+}$  (1.5 equiv.) detection was carried out by adding a mixture of other metal ions and  $Zn^{2+}$  to the sensor solution.

In the IR spectra of XQN, the stretching vibration absorption peaks of amide N-H appeared at  $3473\text{ cm}^{-1}$  (Fig. 5). However, when XQN was coordinated with  $\text{Zn}^{2+}$ , the stretching vibration absorption peak disappeared, because the amide  $\text{O}=\text{C}-\text{N}-\text{H}$  deprotonated and tautomerized to  $\text{C}=\text{N}$ , and a new stretching vibration absorption peaks appeared at  $1666\text{ cm}^{-1}$ . In accordance with the 1:1 stoichiometry, sensor XQN was the most likely to chelate with  $\text{Zn}^{2+}$  via N, O-donor atoms because of the delocalization of  $\text{O}=\text{C}-\text{N}$  group. And a new peak of  $\text{C}=\text{N}$  appeared at  $1629\text{ cm}^{-1}$  because the spiroactam ring opened. For the complex  $[\text{XQN}-\text{Zn}^{2+}]$ , the  $\text{NO}_3^-$  was incorporated and balanced the positive charges of  $\text{Zn}^{2+}$  ion, which was confirmed by the characteristic peak of the  $\text{NO}_3^-$  with the intense band at  $1383\text{ cm}^{-1}$ . Therefore, IR and the Job's plots may suggest that XQN interact with  $\text{Zn}^{2+}$  via N, O-donor atom because of the delocalization of  $\text{O}=\text{C}-\text{N}$  group as shown in Scheme-2.

By the absorption spectrum and the emission spectrum, it showed that the obvious change in color could be watched by naked-eyes. When the spiroactam was closed, it looked colorless. But after  $\text{Zn}^{2+}$  was added in the solution of sensor XQN, the ring was opened and transformed into amide form. So the absorption peak at  $525\text{ nm}$  appeared. And the luminescent peak at  $550\text{ nm}$  was detected. With the concentration of  $\text{Zn}^{2+}$  rising, the absorption peak and emission peak of  $[\text{XQN}-\text{Zn}^{2+}]$  were enhanced. In addition, the detection limits of XQN towards  $\text{Zn}^{2+}$  was calculated as  $2.39\text{ }\mu\text{M}$  (see SI Table S1) [28]. In addition, the comparative analyses of XQN with the previous reported probe were displayed in Table-1. In order to further study the fluorescent properties, the binding constant, the life time and fluorescence quantum yield of  $\text{XQN}-\text{Zn}^{2+}$  was also measured (see SI Table S1).

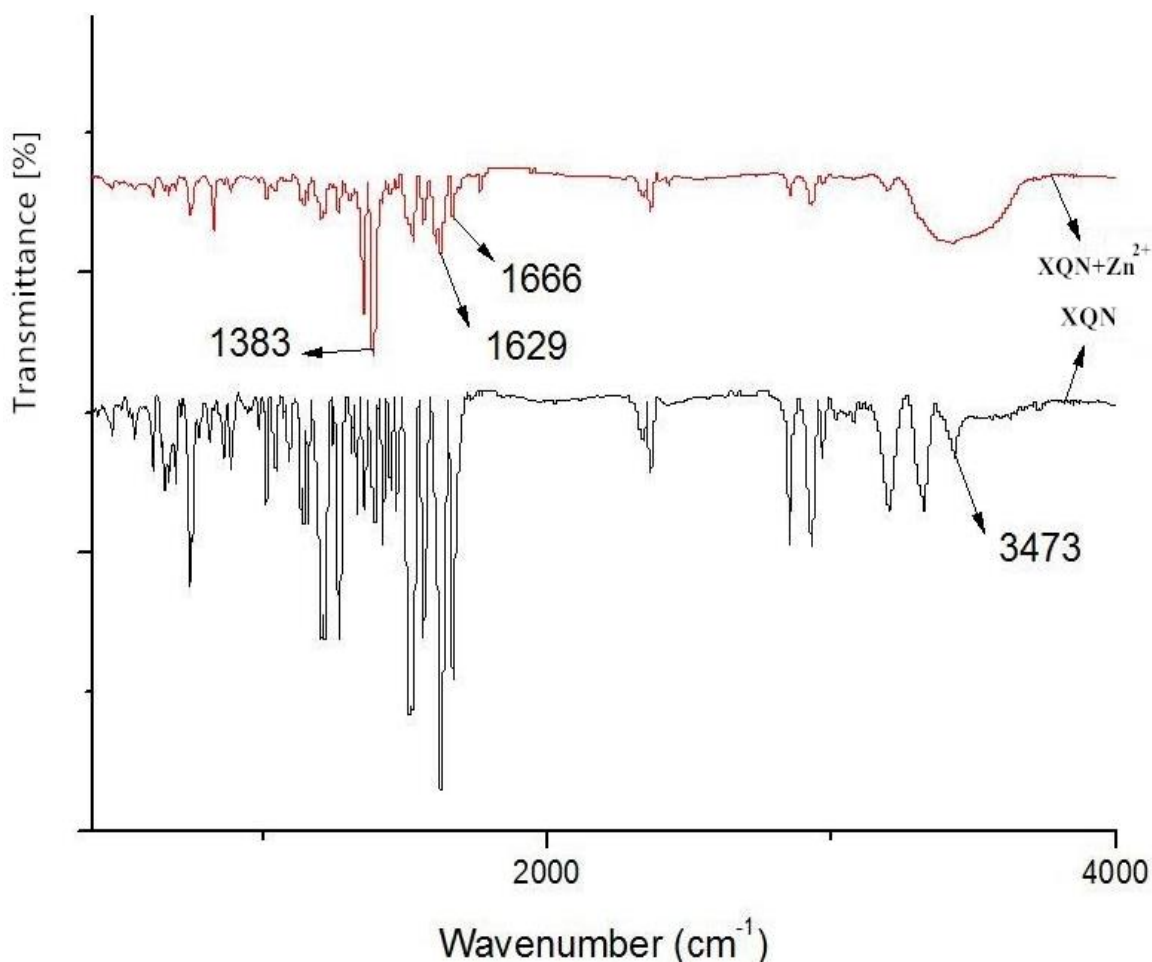
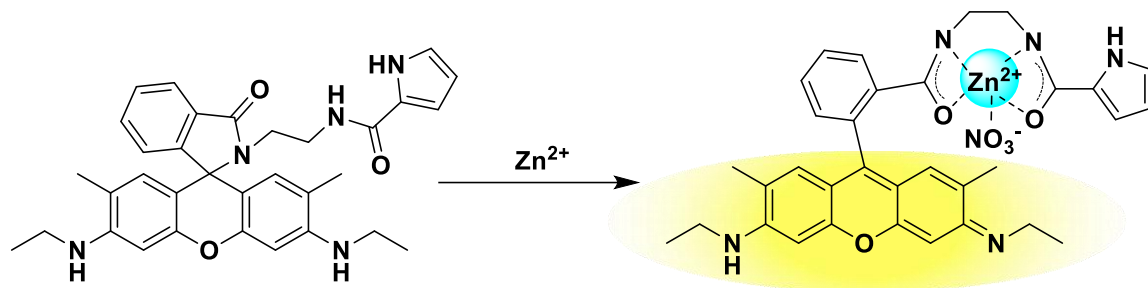
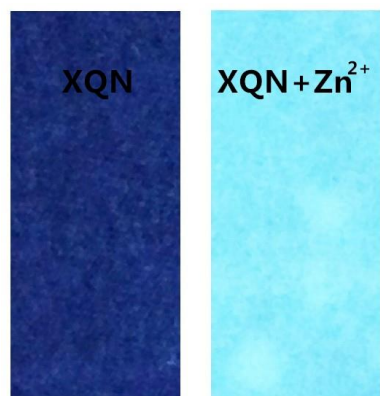


Fig. 5: Comparison between the FT-IR spectral data for XQN and its  $\text{Zn}^{2+}$  complex.

Scheme-2: The proposed mechanism of XQN for Zn<sup>2+</sup> ion.Table-1: Fluorescent sensors reported for the detection of Zn<sup>2+</sup>.

Probe name	Solvent	Detection limit	References
CTS	EtOH/HEPES buffer	5.03×10 <sup>-7</sup> M	[15]
L2	CH <sub>3</sub> CN	1.4×10 <sup>-6</sup> M	[16]
BAR	MeCN-H <sub>2</sub> O	2.21 μM	[17]
This work	CH <sub>3</sub> CN-PBS buffer	2.39 μM	Present work

To investigate the practical application of sensor, test strips were prepared by immersing filter papers into a CH<sub>3</sub>CN-PBS (10 mM, v/v=7:3, pH=7.4) solutions of sensor **XQN** (1×10<sup>-4</sup> M) followed by air drying. Then these test strips were utilized to sense Zn<sup>2+</sup> (1×10<sup>-4</sup> M). As shown in Fig. 6, the obvious color change was observed under the 365 nm UV lamp in the presence of Zn<sup>2+</sup>. So, this study indicated that test strips of **XQN** had the potential to detect Zn<sup>2+</sup> colorimetrically and fluorimetrically in solid state as well.

Fig. 6: Photographs of XQN (1×10<sup>-4</sup> M) on test papers under irradiation at 365 nm.

### Conclusions

In summary, the rhodamine-based sensor **XQN** was synthesized and characterized. The sensor **XQN** exhibited highly selective and sensitive recognition toward Zn<sup>2+</sup> against other metal ions in CH<sub>3</sub>CN-PBS (10 mM, v/v=7:3, pH=7.4) solution. The binding mode was

proposed based on the the Job's plots analyses and IR analysis. Moreover, test strips were prepared by immersing filter papers into the solution of **XQN**, which exhibited good selectivity to Zn<sup>2+</sup>. These findings indicated that sensor **XQN** modified by pyrrole unit had potential applications in physiological and environmental systems for Zn<sup>2+</sup> detection.

### Acknowledgement

This work was supported by the National Natural Science Foundation of China (NSFC) (No. 21302019 and 21171040), the Key Projects of Natural Science Research of Anhui Province Colleges and Universities (No. KJ2018A0338 and No. KJ2018A0337), the Key Projects of Support Program for Outstanding Young Talents in Anhui Province Colleges and Universities (No. gxyqZD2016068), National Undergraduate Training Programs for Innovation and Entrepreneurship (No. 201710371020), the Innovation Training Program for the Anhui College Students (No. 201710371089), and the Key Natural Science Research Projects of Fuyang Normal University (No. 2017FSKJ06ZD), and the Horizontal Cooperation Project of Fuyang Municipal Government-Fuyang Normal University (No. XDHX201730 and No. XDHX201731).

### References

1. J. Li, D. Yim, W. D. Jang and J. Yoon, Recent progress in the design applications of fluorescence probes containing crown ethers, *Chem. Soc. Rev.*, **46**, 2437 (2017)

- H. Moon, J. Park and J. Tae, Fluorescent probes based on rhodamine hydrazides Hydroxamates, *Chem. Rec.*, **16**, 124 (2016).
- Q. Zhang, H. Wei, R. Zhai, Z. Ji, Y. Qi and X. Zhao, 5-(N-Ethylcarbazol-3-yl) thiophene-2-carbaldehyde (ECTC): a novel fluorescent sensor for ferric ion, *Heterocycl. Commun.*, **22**, 287 (2016).
- Y. Wang, H. Wang, X. Zhao, Y. Jin, H. Xiong, J. Yuan and J. Wu, A  $\beta$ -diketonate-europium (III) complex-based fluorescent probe for highly sensitive time-gated luminescence detection of copper sulfide ions in living cells, *New J. Chem.*, **41**, 5981 (2017).
- M. Formica, V. Fusi, L. Giorgi and M. Micheloni, New fluorescent chemosensors for metal ions in solution, *Coord. Chem. Rev.*, **256**, 170 (2012).
- S. Cao, Q. Jin, L. Geng, L. Mu and S. Dong, A "turn-on" fluorescent probe for the detection of  $\text{Cu}^{2+}$  in living cells based on a signaling mechanism of N [double bond, length as m-dash] N isomerization, *New J. Chem.*, **40**, 6264 (2016).
- P. Jiang and Z. Guo, Fluorescent detection of zinc in biological systems: recent development on the design of chemosensors biosensors, *Chem. Rev.*, **248**, 205 (2004).
- E. J. Song, H. Kim, I. H. Hwang, K. B. Kim, A. R. Kim, I. Noh and C. Kim, A single fluorescent chemosensor for multiple target ions: Recognition of  $\text{Zn}^{2+}$  in 100% aqueous solution F in organic solvent, *Sens. Actuators B.*, **195**, 36 (2014).
- S. Karakaya and F. Algi, A novel dual channel responsive zinc (II) probe, *Tetrahedron Lett.*, **55**, 5555 (2014).
- R. K. Pathak, V. K. Hinge, A. Rai, D. Panda and C. P. Rao, Imino-Phenolic-Pyridyl conjugates of Calix[4]arene (L1 L2) as primary fluorescence switch-on sensors for  $\text{Zn}^{2+}$  in solution in HeLa cells the recognition of pyrophosphate ATP by  $[\text{ZnL}_2]$ , *Inorg. Chem.*, **51**, 4994 (2012).
- M. Ahmad, R. Sundari and L. Y. Heng, Development of an optical fibre reflectance sensor for copper (II) detection based on immobilised salicylic acid, *Sens. Actuators B Chem.*, **113**, 201 (2006).
- A. Torrado, G. K. Walkup and B. Imperiali, Exploiting polypeptide motifs for the design of selective Cu (II) ion chemosensors, *J. Am. Chem. Soc.*, **120**, 609 (1998).
- A. Ajayaghosh, P. Carol and S. Sreejith, A ratiometric fluorescence sensor for selective visual sensing of  $\text{Zn}^{2+}$ , *J. Am. Chem. Soc.*, **127**, 14962 (2005).
- C. Li, S. Li and Z. Yang, Development of a coumarin-furan conjugate as  $\text{Zn}^{2+}$  ratiometric fluorescent probe in ethanol-water system, *Spectrochim. Acta. A.*, **174**, 214 (2007).
- J. Zhu, Y. Zhang, Y. Chen, T. Sun, Y. Tang, Y. Huang, Q. Yang, D. Ma, Y. Wang and M. A. Wang, A Schiff base fluorescence probe for highly selective turn-on recognition of  $\text{Zn}^{2+}$ , *Tetrahedron Lett.*, **58**, 365 (2017).
- Z. Kowser, U. Rayhan, S. Rahman, P. E. Georghiou and T. Yamato. A fluorescence "turn-on" sensor for multiple analytes:  $\text{OAc}^- \text{F}^-$  triggered fluorogenic detection of  $\text{Zn}^{2+}$  in a cooperative fashion, *Tetrahedron*, **73**, 5418 (2017).
- S. Erdemir, M. Yuksekogul, S. Karakurt and O. Kocyigit, Dual-channel fluorescent probe based on bisphenol A-rhodamine for  $\text{Zn}^{2+} \text{Hg}^{2+}$  through different signaling mechanisms its bioimaging studies, *Sens. Actuators B Chem.*, **241**, 230 (2017).
- S. Erdemir, O. Kocyigit and S. Karakurt, Dual-channel fluorescent probe based on bisphenol A-rhodamine for  $\text{Zn}^{2+} \text{Hg}^{2+}$  through different signaling mechanisms its bioimaging studies, *Sens. Actuators B Chem.*, **220**, 381 (2015).
- R. Zhang, F. Yan, Y. Huang, D. Kong, Q. Ye, J. Xu and L. Chen, Rhodamine-based ratiometric fluorescent probes based on excitation energy transfer mechanisms: construction applications in ratiometric sensing, *RSC Adv.*, **6**, 50732 (2016).
- O. Sunnapu, N. G. Kotla, B. Maddiboyina, G. S. Asthana, J. Shanmugapriya, K. Sekar and G. Sivaraman, Rhodamine based effective chemosensor for Chromium (III) their application in live cell imaging, *Sens. Actuators B Chem.*, **246**, 761 (2017).
- Y. Wang, H. Q. Chang, W. N. Wu, W. B. Peng, Y. F. Yan, C. M. He, T. T. Chen, X. L. Zhao and Z. Q. Xu, Rhodamine 6G hydrazone bearing pyrrole unit: Ratiometric selective fluorescent sensor for  $\text{Cu}^{2+}$  based on two different approaches, *Sens. Actuators B Chem.*, **228**, 395 (2016).
- X. Q. Hu, J. Chai, Y. F. Liu, B. Liu and B. S. Yang, Probing chromium(III) from chromium(VI) in cells by a fluorescent sensor, *Spectrochim. Acta A.*, **153**, 505 (2016).
- J. Li, C. Yin and F. Huo, Development of fluorescent zinc chemosensors based on various fluorophores their applications in zinc recognition, *Dyes Pigm.*, **131**, 100 (2016).
- P. Puangploy, S. Smanmoo and W. Surareungchai, A new rhodamine derivative-based chemosensor for highly selective sensitive determination of  $\text{Cu}^{2+}$ , *Sens. Actuators B Chem.*, **193**, 679 (2014).
- Z. Yang, Y. Zhao, S. Chen, Y. Bu, X. Zhu, Y. Du and F. Li, A highly sensitive selective colorimetric "Off-On" chemosensor for  $\text{Cu}^{2+}$  in aqueous media based on a rhodamine derivative

- bearing thiophene group, *Sens. Actuators B Chem.*, **235**, 414 (2016).
26. S. Guang, G. Wei, Z. Yan, Y. Zhang, G. Zhao, R. Wu and H. Xu, novel turn-on fluorescent probe for multi-channel detection of  $Zn^{2+}$  and  $Bi^{3+}$  with different action mechanisms, *Analyst*, **143**, 449 (2018).
27. H. Kang, C. Fan, H. Xu, G. Liu and S. Pu, A highly selective fluorescence switch for  $Cu^{2+}$  and  $Fe^{3+}$  based on a new diarylethene with a triazole-linked rhodamine 6G unit. *Tetrahedron*, **74**, 4390 (2018).
28. M. Devi, A. Dhir and C. P. Pradeep, Modulating sensitivity detection mechanism with spacer length: a new series of fluorescent turn on chemodosimeters for  $Pb^{2+}$  based on rhodamine-quinoline conjugates, *RSC Adv.*, **6**, 112728 (2016).